Materials and Structures (2018) 51:80
https://doi.org/10.1617/s11527-018-1208-x

ORIGINAL ARTICLE

Effect of water to cement ratio on the mode III fracture energy of self-compacting concrete

S. Firoozi · M. Dehestani · B. Navayi Neya

Received: 20 December 2017 / Accepted: 6 June 2018

Abstract This paper is an experimental research in order to evaluate the effect of various water to cement (W/C) ratios on the mode III fracture energy of self-compacting concrete. Mix designs with different W/C ratios of 0.45, 0.55 and 0.65 were examined. The experiment was performed on cylindrical specimens of similar geometry and different dimensions, having initial circumferential notch loaded in torsion. In order to calculate the mode III fracture energy of concrete, Bazant's size-effect law was used. The results of the experiment showed that as W/C ratio increased from 0.45 to 0.65, mode III fracture energy of self-compacting concrete decreased by 24%. This difference appears to be due to the porosity and strength reduction of cement paste and the interfacial transition zone at high W/C ratios. It was thus observed that by increasing the W/C ratio, brittleness number is increased.

Keywords Fracture energy · Mode III fracture · Size effect · Self-compacting concrete · Water to cement ratio

S. Firoozi · M. Dehestani (✉) · B. Navayi Neya
Babol Noshirvani University of Technology, Babol, Islamic Republic of Iran
e-mail: dehestani@nit.ac.ir

Published online: 15 June 2018

1 Introduction

Self-compacting concrete (SCC) is a very fluid and highly homogeneous mixture, which eliminates many of the problems of ordinary concrete, such as segregation, bleeding and high permeability, compacting under its own weight without the need for any internal and external vibrators. In cases where it is difficult or impossible to access the casting site, SCC is undoubtedly one of the best alternatives [1–3]. Better surface finish, increased run speed and reduced manpower are of benefits of SCC. For this reason, SCC has been considered by many engineers [4].

Today, the fracture mechanics and specifically the fracture energy induced by the crack propagation and consequently exact and quick inspection of structures has gained a considerable prominence in the industry [5]. The limitations of concrete fracture behavior up to cracking moment and ignoring the crack growth and extension criteria are the most important weaknesses of the design regulations which are used today [6]. As a result, the fracture mechanics, which is the science to investigate the response and failure of structures due to the growth and extension of cracks based upon the energy criterion, is a suitable approach for designing concrete structures.

In the science of fracture mechanics, the deformations in the vicinity of cracks serve as a factor in understanding the type of fracture and its development [7]. Many researches have been performed on fracture

parameters in mode III (antiplane shear failure) for different types of materials.

Suresh and Tschegg [8] tested ceramic samples under combined tensile and torsional loadings. Reardon and Quesnel [9] investigated the effect of interaction of the fracture surface on the torsional stiffness of the steel alloy. Ehart et al. [10], tested wooden specimens of different dimensions under mode III loading. Finally, Qin [11] studied the behavior of piezoelectric materials under antiplane fracture.

Most of the previous researches on the fracture behavior of concrete have been performed in modes I and II fracture of concrete. The mode III fracture of concrete occurs in some locations, such as beams and slabs under torsion, T-beams, balcony slabs, spiral staircases, industrial crane beams, etc. Therefore, the examination of the mode III state appears to be critical [12–14]. In 1987, Bažant and Prat loaded circumferentially-notched cylindrical specimens with similar geometry and different dimensions under torsion, applying the force couple property. They obtained the amount of mode III fracture energy of concrete using Bažant 's size effect law and showed that the mode III fracture energy of concrete is 3 times greater than the mode I fracture energy, 9 times smaller than the mode II fracture energy [15]. In a similar study by Bažant et al. [16], investigating the mode III fracture energy of concrete and mortar confirmed that the fracture behavior of mortar relative to concrete is closer to the behavior of linear fracture mechanics, and the mode III fracture energy to the mode I fracture ratio for the mortar and concrete is equal to 8 and 3, respectively. In 2016, Golewski loaded the cylindrical specimens under pure torsion and calculated the stress intensity factor of the mode III for different values of fly ash. He observed that the addition of fly ash to replace 20% of cement caused an increase in antiplane shear fracture toughness (K_{IIIc}), but adding by 30% fly ash reduced K_{IIIc} [17]. Various methods of applying torsional load have been proposed by researchers [17, 18].

According to previous studies, concrete fracture behavior is affected by materials used in it. Regarding that the constitutive ingredients of normally vibrated concrete (NVC) differ with SCC, many fracture characteristics of these two concretes will be different. On the other hand, W/C plays a vital role in the mechanical properties of concrete. Many studies have been conducted on the effect of W/C on fracture parameters:

Petersson [19] concluded that an important factor in the fracture energy of NVC is the water to cement ratio. Nallathambi et al. [20] indicated that by increasing W/C ratio, the fracture toughness of the NVC concrete was significantly reduced and this provided some appropriate empirical relations. Wittmann et al. [21] investigated the effect of age, loading rate and water to cement ratio on the fracture energy of NVC concrete in 1987, and observed that the amount of fracture energy decreased, when the water to cement ratio increases. Jo and Tae [22], studying the mode I fracture energy, found that reducing W/C increased the fracture energy. Carpinteri and Brighenti [23] loaded initially notched concrete specimens subjected to three-point bending and concluded that a ratio of W/C slightly higher than the minimum amount required for the cement hydration process, could produce optimal fracture energy values. Beygi et al. estimated the fracture parameters for SCC with a different W/C ratio in 2013, using the work-of-fracture method (WFM) and the size-effect method (SEM), and stated that as W/C decreased from 0.7 to 0.35 in self-compacting concrete, the fracture toughness increased linearly and the fracture brittleness is approximately doubled [24].

Despite recent efforts and due to the lack of information concerning the fracture parameters of SCC, the study of the mode III fracture energy of SCC and the assessment of W/C effect on the mode III fracture energy is necessary. In this research, using the same samples as Bažant and Prat [15] applied Bažant's size effect relation, the mode III fracture energy of SCC for the water to cement ratios of 0.45, 0.55 and 0.65 is obtained. The mode III fracture energy relation was proposed in terms of compressive strength with good accuracy and the brittleness number for different W/C ratios was calculated.

2 Experimental program

2.1 Materials and mix designs

In the present study, three mixes were designed with W/C ratios of 0.45, 0.55 and 0.65. Crushed stones with the maximum grain size of 12.5 mm was used in this study according to the ASTM standard of grading

curve. The sand in all mix designs is crushed sand with a maximum grain size of 9.5 mm, a fineness modulus of 2.8 and a sand equivalent value SE = 80%. Gradation curve of fine and coarse aggregate along with the ASTM C33 standard range is shown in Fig. 1.

Type II Portland cement made by Mazandaran cement factory was used in this study. Limestone powder, produced by Negin factory of Neka (Iran) with a specific gravity of 2666 kg/m^3, was used to increase the viscosity of the SCC. Superplasticizer (SP) of carboxylate base type, provided by Namikaran Company, was used for the flowability of the SCC.

In order to attain a homogeneous mixture of SCC, all materials were mixed over a period of 5–6 min. After mixing, to test the properties of fresh concrete, slump flow, flow time (T50) and L-box tests were performed according to the EFNARC recommendations [25]. The mix designs and the flow properties of the fresh concrete are listed in Table 1.

Table 1 Mix designs and fresh properties of the concrete

Material	S1	S2	S3
Cement (C) (kg/m^3)	350	335	320
Gravel (kg/m^3)	790	790	790
Sand (kg/m^3)	680	680	680
Limestone powder (P) (kg/m^3)	350	350	350
Free water (W) (kg/m^3)	157.50	184.25	208
Superplasticizer (kg/m^3)	3.89	1.95	1.64
W/C (by weight)	0.45	0.55	0.65
W/P (by weight)	0.23	0.27	0.31
Unit weight (kg/m^3)	2331	2341	2350
Slump flow (mm)	730	685	690
T_{50} (s)	4.99	4.46	3.93
L-box (h_2/h_1)	0.92	0.88	0.86

2.2 Preparation of test specimens and test setup

In order to assess the effect of W/C on the mode III fracture energy of SCC, the test was accomplished on circumferentially notched cylindrical specimens with similar geometry and different dimensions. The cylindrical samples were made of compressed plastic molds (Ertalon), which do not have any water absorption. The geometric characteristics of the notched cylindrical samples are shown in Fig. 2. The diameters of the cylinders were d = 38.1, 76.2, and 152.4 mm. The length to diameter ratio of the specimens is $\frac{l}{d} = 2$ and the circumferential notch with a thickness of $^1/_{16}$ in. is placed in the middle of specimens. The initial notch length of all samples is $a_0 = \frac{d}{4}$. As shown in Fig. 2, opposite couples were applied at two ends of cylindrical specimens with an arm of $\frac{2d}{3}$ to create a pure torsion (T).

In addition to the torsional tests on the notched cylindrical samples, 12 standard cylindrical samples of 150 mm × 300 mm were made for each mix and cured under water at temperature 22 °C. These samples were used to determine the compressive strength, f'_c, the splitting tensile strength, f'_t, the elastic modulus, E_c, and the Poisson's ratio, ν of the mix designs based on ASTM: C 469, ASTM: C 496, ASTM: C 39 [26–28]. To this end, at least 3 specimens were considered for each test (Fig. 3). All cylindrical specimens were loaded in a closed loop servo electro

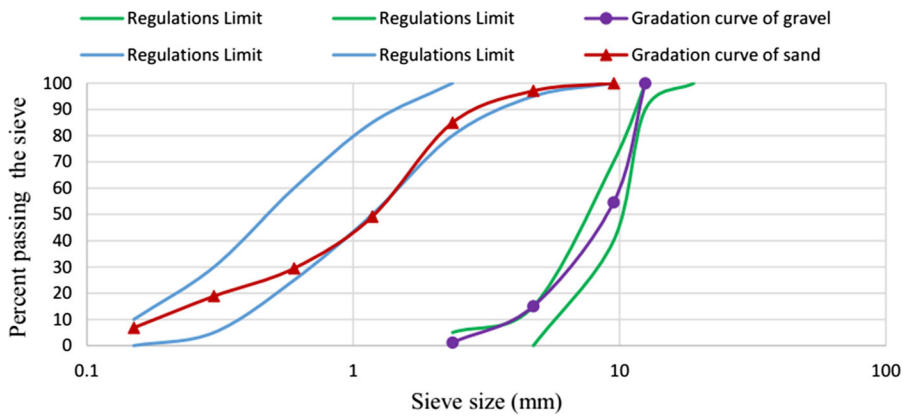

Fig. 1 Gradation curves of fine and coarse aggregates

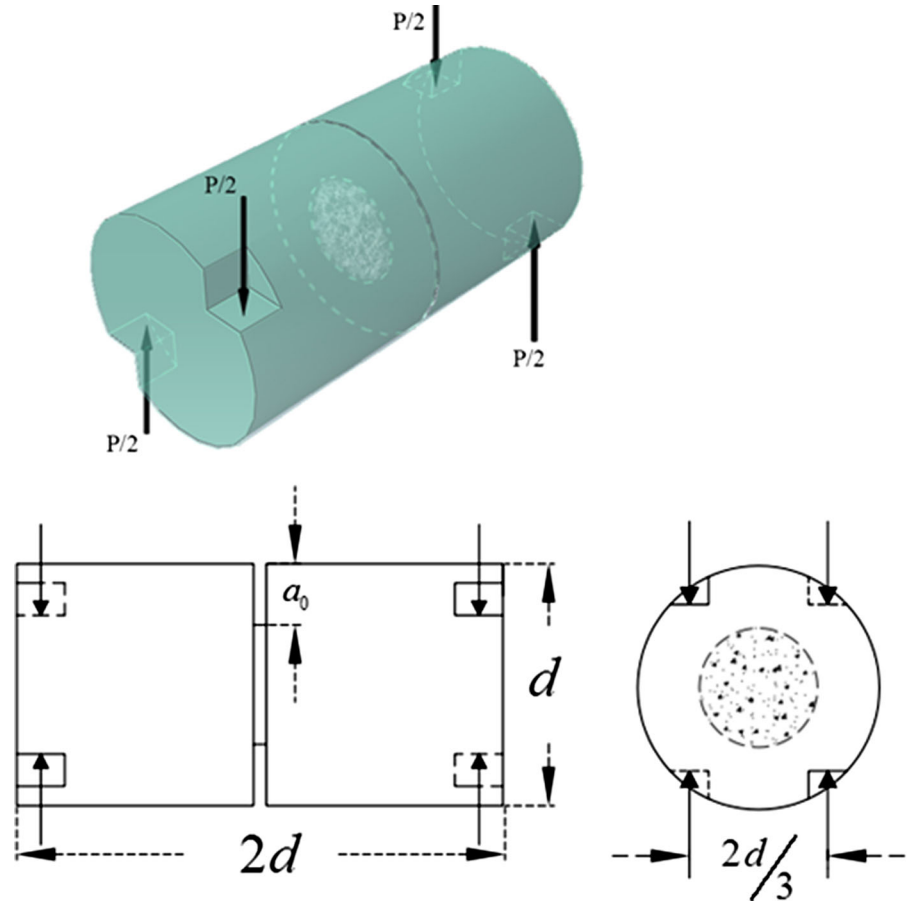

Fig. 2 Torsional circumferentially notched specimens

Fig. 3 Tested specimens with different dimensions

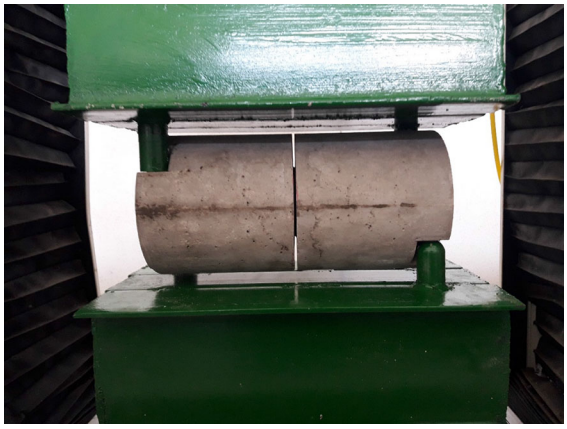

Fig. 4 A typical loaded specimen

controlled testing universal machine with a maximal capacity of 400 kN and a constant displacement rate. The device loading rate was chosen so that all specimens would reach the maximum load within 3–5 min. Figure 4 shows the arrangement of sample below the device.

2.3 Calculating fracture energy G_f^{III}

The fracture energy G_f^{III}, known the total energy, is indeed the energy required to extend a crack with a unit length. In order to calculate the mode III fracture energy of concrete, Bažant's size effect law is used. To consider the size effect in the fracture mechanics, Bažant proposed that the released energy during fracture is a function of the dimensions of structure and the size of damaged zone of the crack tip. Based on Bažant's size effect law, this yields [29]:

$$\tau_n = Bf_t'\left[1+\frac{d}{\lambda_0 d_a}\right]^{-1/2} \quad (1)$$

where τ_n is the nominal stress at failure, and in the general case $\tau_n = \frac{CP}{d^2}$, P = maximum load, d = characteristic dimension of the specimen, C = arbitrary nondimensional constant. For the specimens used in the present study, $\tau_n = \frac{16T}{\pi d^3}$ in which T = maximum applied torque, B and λ_0 are empirical constants obtained by experiment, f_t' the tensile strength, and d_a is the maximum size of aggregate. Furthermore, Bažant's size effect was presented theoretically for two-dimensional and three-dimensional problems by Bažant [30, 31]. Many researches have been conducted on the size effect which emphasize the practical approach of this relation [32–35].

Simplifying Eq. (1) gives:

$$\left[\frac{f_t'}{\tau_n}\right]^2 = \frac{1}{B^2\lambda}\frac{d}{d_a}+\frac{1}{B^2} \quad (2)$$

It is observed, by examining Eq. (2) that there is a linear relation between $\left[\frac{f_t'}{\tau_n}\right]^2$ and $\frac{d}{d_a}$, hence:

$$Y = AX + C \quad (3)$$

where $A = \frac{1}{B^2\lambda_0}$ and $C = \frac{1}{B^2}$. The constants A and C may be obtained by linear regression of the test results and consequently the empirical constants B and λ_0 are calculated.

In structures where the dimensions to the maximum aggregate size ratio is small, in Eq. (1), the term $\frac{d}{\lambda_0 d_a}$ after the number 1, can be neglected, and Eq. (1) yields $\tau_n = Bf_t'$. Therefore, it can be seen that the strength criterion holds for small structures. For structures with large proportion of dimensions to the maximum aggregate size, the number 1 in front of $\frac{d}{\lambda_0 d_a}$ can be omitted which gives $\tau_n = Bf_t'\left(\frac{d}{\lambda_0 d_a}\right)^{-1/2}$. It is seen that for the large concrete structures, the linear elastic fracture mechanics (LEFM) criteria is dominant.

The curve Log (τ_n/Bf_t') versus Log $(d/\lambda_0 d_a)$ is plotted in order to examine the size effect law. It can be shown that there is a nonlinear relation between the specimen size and the nominal strength [30].

The mode III fracture energy in this study is computed as the following equation [31, 36, 37]:

$$G_f = \frac{g(\alpha_0)}{AE_c}f_t'^2 d_a \quad (4)$$

where $\alpha_0 = \frac{a_0}{r}$, a_0 is the notch length, r is the radius of the cylinder, E_c is the elastic modulus of concrete, f_t' is the direct tensile strength, $A = \frac{1}{B^2\lambda_0}$ is the slope of the regression line in Eq. (6), $g(\alpha_0)$ is the energy release rate and d_a is the maximum size of aggregate.

According to references [15, 38, 39] for notch length $a_0 = d/4$, $g(\alpha_0) = 6.99(1+\nu)$, where ν is the Poisson's ratio.

Moreover, in the size effect method, the adjacency of the material fracture behavior to the LEFM behavior is determined by the parameter β, which is suggested by Bažant and Kazemi [15, 40]:

$$\beta = \frac{d}{\lambda_0 d_a} \quad (5)$$

where β is the brittleness number. When $\beta \le 0.1$, the behavior of the structure is more ductile and the nominal strength of the structure is constant, which corresponds to the yield limit, while for values of $\beta \ge 10$, the behavior of the structure is more brittle and the nominal strength is proportional to $d^{-0.5}$, as suggested by LEFM. Besides, if $0.1 \le \beta \le 10$, nonlinear fracture mechanics (NLFM) will govern.

3 Test results and evaluation

3.1 Mechanical properties

Table 2 shows the mechanical properties for different water to cement ratios of the SCC. It is clear that the water to cement ratio plays a critical role in the mechanical properties of SCC. The results show that with the increase of the water to cement ratio from

Table 2 Mechanical properties of concrete

Mix no.	W/C	f_c (MPa)	f_t (MPa)	E (GPa)	v
S1	0.45	53.50	4.17	34.10	0.19
S2	0.55	33.07	4.10	27.90	0.19
S3	0.65	26.43	3.59	23.90	0.18

0.45 to 0.65, the compressive strength decreases by 50%. Similar results have been reported by Rao [41], Fernandes et al. [42] and Nikbin et al. [43]. Increasing the W/C ratio results in an increase in water among the concrete particles and the presence of this excess water will cause porosity in hardened concrete, which affects the compressive strength and fracture energy of concrete.

Examining the results, declares that with an increase in water to cement ratio from 0.45 to 0.65, the splitting tensile strength decreases by 14%. Siddique et al. [44] and Nikbin et al. [43] in a similar experiment indicated that by increasing W/C, the tensile strength decreases. According to previous studies, the tensile strength was assumed to be 0.9 times the splitting tensile strength [45].

Additionally, by studying the results, as the water to cement ratio increases from 0.45 to 0.65, the modulus of elasticity decreases by 30%. In the researches performed by Haach et al. [46] and Nikbin et al. [43] similar results were achieved.

3.2 Fracture energy G_f^{III}

Since most of the previous researches were carried out on the modes I and II fracture energy, there is no comprehensive information on the effect of W/C ratio on the mode III fracture energy of SCC. Many previous studies, that investigated the effect of water to cement ratio on the mode I fracture energy of concrete, stressed that increasing water to cement ratio resulted in a decrease in the amount of energy in the mode I fracture energy of concrete [24, 47, 48].

In order to calculate the mode III fracture energy of SCC the maximum load diagrams applied to the specimens are shown in Fig. 5 in terms of vertical displacements of device. The maximum torsional values applied to the specimens are given in Table 3. By measuring the maximum applied torsion, T, $\tau_n = \frac{16T}{\pi d^3}$ was calculated and the parameters A and C were

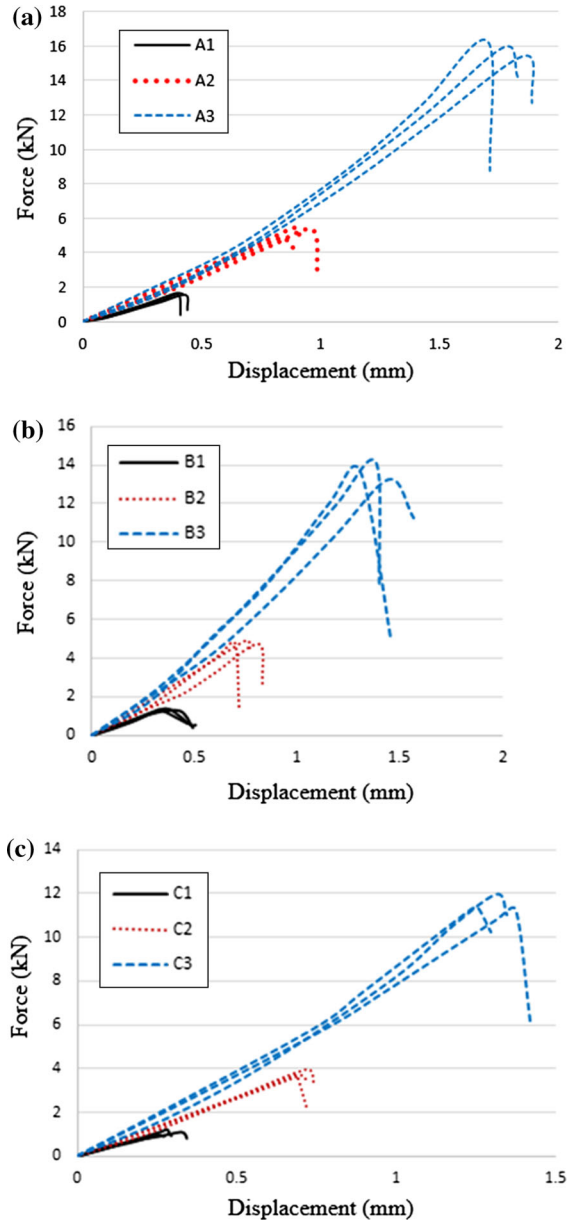

Fig. 5 Maximum loads: **a** W/C = 0.45; **b** W/C = 0.55; **c** W/C = 0.65

obtained by using linear regression on the test results based on Eq. (3); subsequently the empirical values B and λ_0 were computed.

Figure 6 shows the linear regression on the test results for different W/C ratios. Figure 7 illustrates the size effect of the SCC design with various W/C ratios, and it can be seen that the measured τ_n values are in good agreement with the size effect law. As shown in

Table 3 Maximum torsion

Mix no.	Series	d (mm)	a_0/d	L/d	Corrected maximum load P (N)			Average max. load (N)	Coefficient of variation (%)	Average max. torque (N m)
					Sample 1	Sample 2	Sample 3			
S1	A1	38.1	0.25	2	1640	1564	1530	1578	3.6	20.04
	A2	76.2			5259	5236	5483	5327	2.6	135.28
	A3	152.4			15,437	15,673	16,236	15,782	2.6	801.73
S2	B1	38.1	0.25	2	1275	1331	1364	1323	3.4	16.81
	B2	76.2			4930	4531	4791	4750	4.3	120.67
	B3	152.4			13,169	14,117	13,573	13,620	3.5	691.90
S3	C1	38.1	0.25	2	1220	1074	1117	1137	6.6	14.40
	C2	76.2			3580	3650	3944	3724	5.2	94.60
	C3	152.4			11,874	11,354	11,044	11,424	3.7	580.30

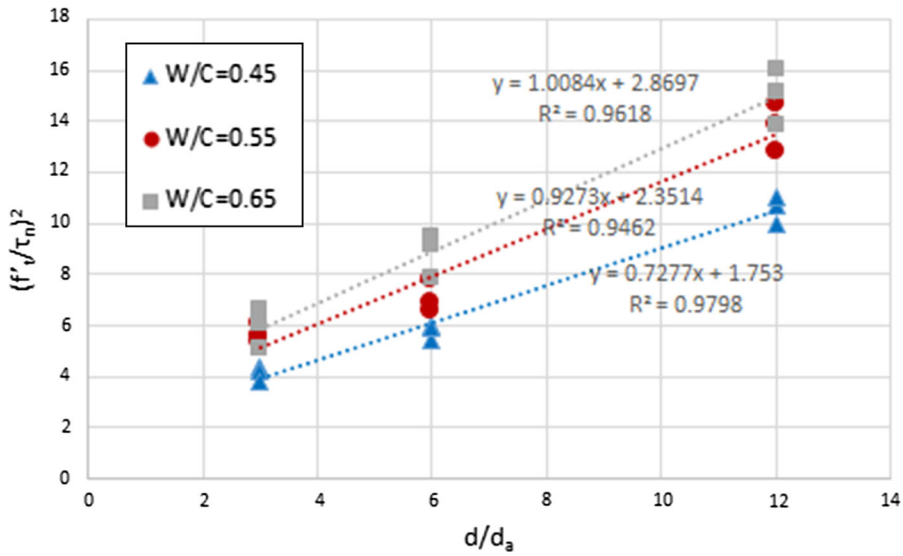

Fig. 6 Linear regressions for SCC mixes

Fig. 7, by decreasing the W/C ratio, the concrete behavior approaches the LEFM line. Figure 8 demonstrates the fracture surface of the broken samples after the test. In the current study, the values for different water to cement ratios were calculated according to Eq. (4). It was observed that with the increase of the water to cement ratio from 0.45 to 0.65, the mode III fracture energy of the SCC decreased by 24% (Fig. 9). Considering previous studies, the porosity in concrete is reduced by decreasing the W/C ratio. Along with porosity reduction, the strength of the cement paste and the interfacial transition zone (ITZ) significantly increases. Increasing the strength of the cement paste, at lower W/C ratios, causes the cracking to propagate across the aggregate and increases the fracture energy [49, 50].

The mechanism of in fracture in mode I is completely different from those of modes II and III. Fracture in mode I is due to normal tensile stresses on the fracture surface, which imposes a predetermined cracking path. However, in modes II and III, the crack propagation is due to the increase in in-plane and out-plane shear stresses, respectively.

In shear and when the specimens are twisted, the microcracks in fracture process zone are inclined to the fracture plane and unlike the mode I, they do not lie

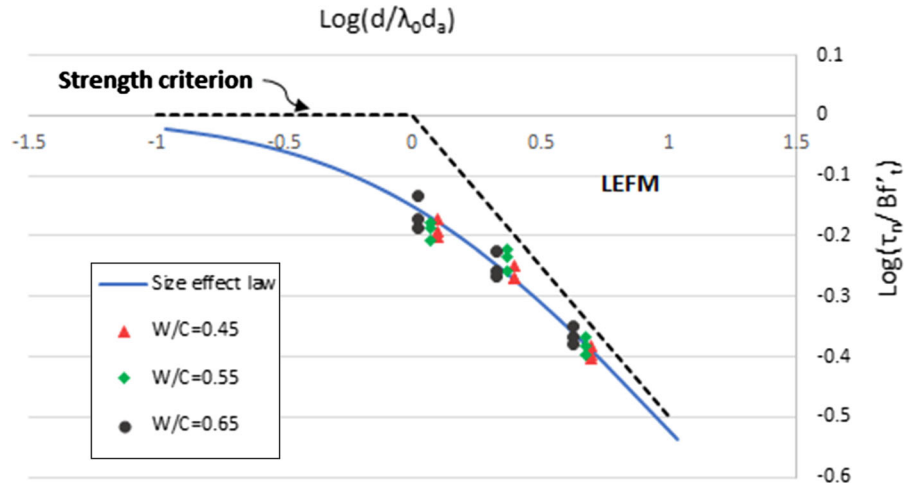

Fig. 7 Size effect for SCC mixes

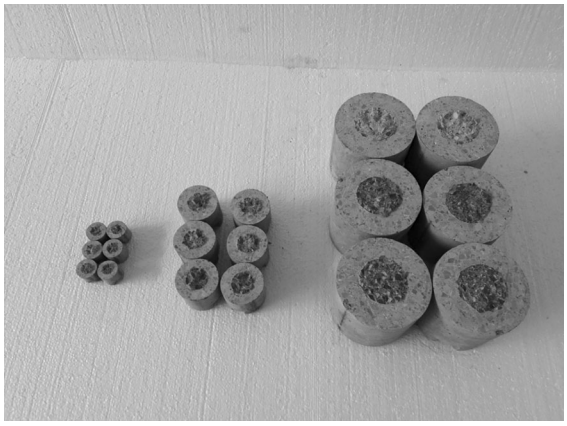

Fig. 8 Fracture surfaces of the broken specimens after the test

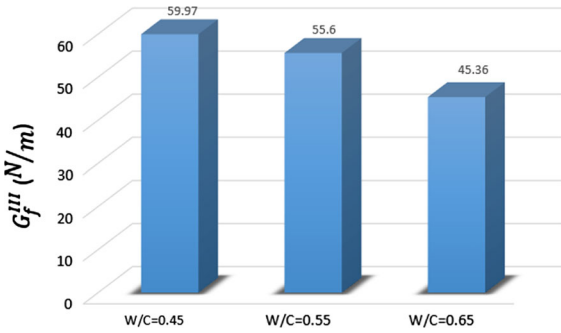

Fig. 9 Mode III fracture energy of the concrete with respect to W/C ratio

in the fracture plane. The intact material between adjacent inclined cracks carries compression force. The reason that one gets very different effective values of the mode III fracture energy of SCC with different W/C ratios can be found in the intact material between cracks. By reducing the proportion of water to cement, the porosity of the concrete decreases and the strength of the cement paste increases, so that, more energy is needed to expand the crack in the intact material.

According to Fig. 9, the growth rate of compressive strength is more pronounced than the growth of the mode III fracture energy of concrete. Also, according to previous studies, the mode III fracture energy of SCC can be estimated in terms of compressive strength with an exponential function [51]. Based on experimental results, a relation between f_c' and G_f^{III} with a correlation coefficient of 0.83 was obtained as:

$$G_f^{III} = 14.757 f_c'^{0.3582} \quad (6)$$

where f_c' is the characteristic compressive strength of SCC in MPa and G_f^{III} is in terms of N/m. The

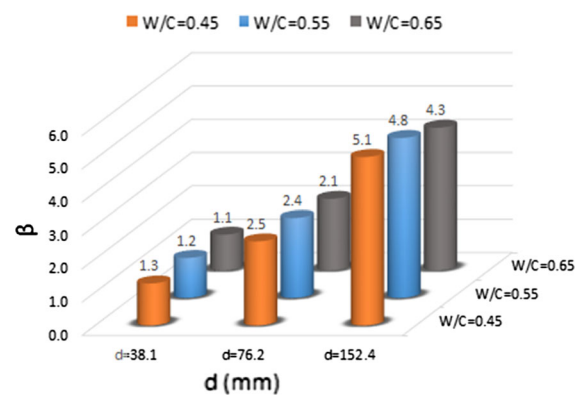

Fig. 10 Variations of brittleness at different dimensions for various W/C ratios

brittleness number, β is calculated using Eq. (5). It can be observed by examining Fig. 10 that by reducing W/C ratio, the SCC concrete will have a more brittle behavior. Bažant and Kazemi [40] indicated that β describes the fracture pattern of a member or structure as well as the design criteria. As it can be seen, all data are in the range of nonlinear fracture mechanics.

4 Conclusions

This research has experimentally examined the effect of various water to cement ratios on the mode III fracture energy of the self-compacting concrete. Accordingly results can be summarized as follows:

(1) By examining the results, it can be concluded that the use of torsional cylindrical specimens having initial circumferential notches, is an appropriate and a reasonable alternative for the determination of the mode III fracture energy of concrete.
(2) The results show that by increasing water to cement ratio from 0.45 to 0.65, the amount of the mode III fracture energy of the SCC decreases by 24%.
(3) By comparing the brittleness number, the SCC will behave more brittle if the W/C ratio decreases.
(4) According to Bažant's size effect curve, it can be stated that by decreasing the W/C ratio, the behavior of the SCC approaches the LEFM line.
(5) The proposed relation was presented with the acceptable precision between the mode III fracture energy of the SCC and the compressive strength of the specimen.

Acknowledgements Authors would like to appreciate the faculty members of Faculty of Civil Engineering at Babol Noshirvani Univeresity of Technology of Iran who kindly conducted the research and suggested useful comments and modifications.

Compliance with ethical standards

Conflict of interest The authors declare that they have no conflict of interest.

References

1. Ouchi M, Hibino M, Okamura H (1997) Effect of superplasticizer on self-compactability of fresh concrete. Transp Res Rec J Transp Res Board 1574:37–40
2. Khayat KH (1999) Workability, testing, and performance of self-consolidating concrete. Mater J 96(3):346–353
3. Safiuddin M, West JS, Soudki KA (2011) Flowing ability of the mortars formulated from self-compacting concretes incorporating rice husk ash. Constr Build Mater 25(2):973–978
4. Okamura H, Ouchi M (2003) Self-compacting concrete. J Adv Concr Technol 1(1):5–15
5. Bažant ZP, Planas J (1997) Fracture and size effect in concrete and other quasibrittle materials, vol 16. CRC Press, Boca Raton
6. Parker ER (1957) Brittle behaviour of engineering structures. Wiley, Hoboken
7. Gdoutos EE (2005) Fracture mechanics: an introduction, vol 123. Springer, Netherlands
8. Suresh S, Tschegg EK (1987) Combined mode I–mode III fracture of fatigue-precracked alumina. J Am Ceram Soc 70(10):726–733
9. Reardon AC, Quesnel DJ (1995) Fracture surface interference effects in mode III. Mech Mater 19(2–3):213–226
10. Ehart RJA, Stanzl-Tschegg SE, Tschegg EK (1998) Crack face interaction and mixed mode fracture of wood composites during mode III loading. Eng Fract Mech 61(2):253–278
11. Qin QH (2005) Mode III fracture analysis of piezoelectric materials by Trefftz BEM. Structural Engineering and Mechanics 20(2):225–239
12. Rahal KN (2001) Analysis and design for torsion in reinforced and prestressed concrete beams. Struct Eng Mech 11(6):575–590
13. Kamiński M, Pawlak W (2011) Load capacity and stiffness of angular cross section reinforced concrete beams under torsion. Arch Civ Mech Eng 11(4):885–903
14. Lopes AV, Lopes SM, do Carmo RN (2014) Stiffness of reinforced concrete slabs subjected to torsion. Mater Struct 47(1–2):227–238
15. Bažant ZP, Prat PC (1988) Measurement of mode III fracture energy of concrete. Nucl Eng Des 106(1):1–8
16. Bazant ZP, Prat PC, Tabbara MR (1990) Antiplane shear fracture tests (Mode III). ACI Mater J 87(1):12–19
17. Golewski GL (2017) Determination of fracture toughness in concretes containing siliceous fly ash during mode III loading. Struct Eng Mech 62(1):1–9
18. Luong MP (1992) Fracture testing of concrete and rock materials. Nucl Eng Des 133(1):83–95
19. Petersson PE (1980) Fracture energy of concrete: practical performance and experimental results. Cem Concr Res 10(1):91–101
20. Nallathambi P, Karihaloo BL, Heaton BS (1984) Effect of specimen and crack sizes, water/cement ratio and coarse aggregate texture upon fracture toughness of concrete. Mag Concr Res 36(129):227–236
21. Wittmann FH, Roelfstra PE, Mihashi H, Huang YY, Zhang XH, Nomura N (1987) Influence of age of loading, water–

cement ratio and rate of loading on fracture energy of concrete. Mater Struct 20(2):103–110
22. Jo BW, Tae GH (2001) Experimental study on fracture energy of low-heat concrete by three-point bend tests. Russ J Nondestr Test 37(12):907–915
23. Carpinteri A, Brighenti R (2010) Fracture behaviour of plain and fiber-reinforced concrete with different water content under mixed mode loading. Mater Des 31(4):2032–2042
24. Beygi MH, Kazemi MT, Nikbin IM, Amiri JV (2013) The effect of water to cement ratio on fracture parameters and brittleness of self-compacting concrete. Mater Des 50:267–276
25. EFNARC S (2002) Guidelines for self-compacting concrete. Association House, London, UK, 32:34
26. ASTM C. 39 (2001) Standard test method for compressive strength of cylindrical concrete specimens. ASTM International, West Conshohocken
27. ASTM C. 496 (2004) Standard test method for splitting tensile strength of cylindrical concrete specimens. ASTM International, West Conshohocken
28. ASTM A. C469/C469 M-14 (2014) Standard test method for static modulus of elasticity and Poisson's ratio of concrete in compression. ASTM International, West Conshohocken
29. Bažant ZP (1985) Fracture mechanics and strain-softening of concrete. Preprints, U.S.-Japan seminar on finite element analysis of reinforced concrete structures, Japan Society for the Promotion of Science, Tokyo, May 1985, pp 71–92
30. Bažant ZP (1984) Size effect in blunt fracture: concrete, rock, metal. J Eng Mech 110(4):518–535
31. Bažant ZP (1989) Fracture energy of heterogeneous materials and similitude. In: Shah SP, Swartz SE (eds) Fracture of concrete and rock. Springer, New York, pp 229–241
32. Bažant ZP, Şener S (1987) Size effect in torsional failure of concrete beams. J Struct Eng 113(10):2125–2136
33. Bažant ZP, Cao Z (1987) Size effect in punching shear failure of slabs. ACI Struct J 84(1):44–53
34. Kim JK, Yi ST, Yang EI (2000) Size effect on flexural compressive strength of concrete specimens. Struct J 97(2):291–296
35. Dönmez A, Bažant ZP (2017) Size effect on punching strength of reinforced concrete slabs with and without shear reinforcement. ACI Struct J 114(4):875
36. Bažant ZP, Kim JK, Pfeiffer PA (1986) Nonlinear fracture properties from size effect tests. J Struct Eng 112(2):289–307
37. Bažant ZP, Pfeiffer PA (1987) Fracture energy of concrete: its definition and determination from size effect test. ACI Spec Publ 100:89–110
38. Benthem JP, Koiter WT (1973) Asymptotic approximations to crack problems. In: Sih GC (ed) Methods of analysis and solutions of crack problems. Springer, Dordrecht, pp 131–178
39. Tada H, Paris PC, Irwin GR (1973) The stress analysis of cracks. Del Research Corporation, Handbook
40. Bažant ZP, Kazemi MT (1990) Determination of fracture energy, process zone longth and brittleness number from size effect, with application to rock and conerete. Int J Fract 44(2):111–131
41. Rao GA (2001) Generalization of Abrams' law for cement mortars. Cem Concr Res 31(3):495–502
42. Fernandes V, Silva L, Ferreira VM, Labrincha JA (2005) Evaluation of mixing and application process parameters of single-coat mortars. Cem Concr Res 35(5):836–841
43. Nikbin IM, Beygi MHA, Kazemi MT, Amiri JV, Rabbanifar S, Rahmani E, Rahimi S (2014) A comprehensive investigation into the effect of water to cement ratio and powder content on mechanical properties of self-compacting concrete. Constr Build Mater 57:69–80
44. Siddique R, Aggarwal P, Aggarwal Y (2012) Influence of water/powder ratio on strength properties of self-compacting concrete containing coal fly ash and bottom ash. Constr Build Mater 29:73–81
45. Alhussainy F, Hasan HA, Rogic S, Sheikh MN, Hadi MN (2016) Direct tensile testing of self-compacting concrete. Constr Build Mater 112:903–906
46. Haach VG, Vasconcelos G, Lourenço PB (2011) Influence of aggregates grading and water/cement ratio in workability and hardened properties of mortars. Constr Build Mater 25(6):2980–2987
47. Giaccio G, Rocco C, Zerbino R (1993) The fracture energy (G F) of high-strength concretes. Mater Struct 26(7):381–386
48. Bharatkumar BH, Raghuprasad BK, Ramachandramurthy DS, Narayanan R, Gopalakrishnan S (2005) Effect of fly ash and slag on the fracture characteristics of high performance concrete. Mater Struct 38(1):63–72
49. Elsharief A, Cohen MD, Olek J (2003) Influence of aggregate size, water cement ratio and age on the microstructure of the interfacial transition zone. Cem Concr Res 33(11):1837–1849
50. Akçaoğlu T, Tokyay M, Çelik T (2004) Effect of coarse aggregate size and matrix quality on ITZ and failure behavior of concrete under uniaxial compression. Cem Concr Compos 26(6):633–638
51. Code CFM (1993) Comite Euro-International du Beton. Bulletin d'Information 213:214